

Role of an interfacial FeO layer in the electric-field-driven switching of magnetocrystalline anisotropy at the Fe/MgO interface

Kohji Nakamura,* Toru Akiyama, and Tomonori Ito

Department of Physics Engineering, Mie University, Tsu, Mie 514-8507, Japan

M. Weinert

Department of Physics, University of Wisconsin–Milwaukee, Milwaukee, Wisconsin 53201, USA

A. J. Freeman

Department of Physics and Astronomy, Northwestern University, Evanston, Illinois 60208, USA

(Received 19 May 2010; published 22 June 2010)

The electric-field-induced switching of magnetocrystalline anisotropy (MCA) between in-plane and out-of-plane orientations is investigated by first-principles calculations for the prototypical Fe on MgO(001) system. Our results predict that an ideal abrupt Fe/MgO interface gives rise to a large out-of-plane MCA due to weak Fe-O hybridization at the interface, but the MCA switching by an applied electric field is found to be difficult to achieve. Instead, the existence of an interfacial FeO layer plays a key role in demonstrating the MCA switching that accompanies an electric-field-induced displacement of Fe atoms on the interfacial FeO layer.

DOI: [10.1103/PhysRevB.81.220409](https://doi.org/10.1103/PhysRevB.81.220409)

PACS number(s): 75.30.Gw, 75.70.Cn, 73.20.-r, 75.85.+t

Controlling magnetic properties by means of applied electric field (E field) is a key challenge in materials physics. Materials being studied include magnetoelectric multiferroics^{1–4} and magnetic semiconductors.^{5–7} Even in itinerant thin films, magnetic properties such as the magnetocrystalline anisotropy (MCA) are modified by application of a voltage;⁸ there is general consensus that modification of the surface d -electron charge/spin density induced by the E field contributes to the effect.^{9–12}

Magnetic metal-oxide junctions are seen as an important avenue toward ultrahigh density and nonvolatile electronics^{13,14} needed for information processing and storage technologies. Recent experiments have reported that the perpendicular MCA energy is significantly reduced by an applied voltage in Au/Fe/MgO junctions,¹⁵ i.e., at ultrathin Fe/MgO interfaces. Moreover, the direct switching from out of plane to in plane has been achieved in Au/Fe_{0.8}Co_{0.2}/MgO.¹⁶ Such E -field-driven MCA switching offers a pathway to control magnetism at the nanoscale with ultralow-energy power consumption compared to traditional switching using magnetic fields. Despite its importance, an understanding of the underlying physics and mechanism of the E -field-driven MCA modification in metal-oxide interfaces is still lacking due to the structural and electronic complexity of the interfaces, thus, hindering the search for other promising metal-oxide interface candidates.

Here, we present a mechanism for the E -field-driven MCA modification at the Fe/MgO interface, based on full-potential linearized augmented plane-wave (FLAPW) calculations.^{17,18} These calculations predict that an ideal abrupt Fe/MgO interface gives rise to a large out-of-plane MCA due to weak Fe-O hybridization at the interface, and that the MCA modification is caused by changes in the d -band structure at the Fermi level (E_F) when an E field is introduced. However, the MCA switching by an applied E field is found to be difficult to achieve. Instead, the existence of an interfacial FeO_x layer between the metallic Fe layer and

the MgO substrate plays a key role in facilitating the MCA switching, which accompanies an E -field-induced displacement of the Fe atoms in the interfacial FeO layer.

Calculations were performed using the FLAPW method which treats a single slab geometry^{17,18} that allows a natural way to include an external E field.^{10,19} The E -field potential applied along the surface normal (z axis), $v_{\text{ext}} = F_{\text{ext}}z$, is expanded into interstitial, muffin-tin (MT) spheres and vacuum regions, where F_{ext} and z are the external E -field and z -axis position, respectively.¹⁰ The added v_{ext} is included self-consistently in calculations which are done within the local-spin-density approximation²⁰ and the scalar relativistic approximation (SRA), i.e., excluding the spin-orbit coupling (SOC). LAPW functions with a cutoff of $|\mathbf{k} + \mathbf{G}| \leq 3.9$ a.u. and MT sphere radii of 2.30, 2.15, and 1.80 a.u. for Fe, Mg, and O atoms are used, where the angular-momentum expansion inside the MT spheres is truncated at $\ell = 8$ for the wave functions, charge and spin densities, and potential.

To determine the MCA, the second variational method^{21,22} for treating the SOC is performed by using the calculated eigenvectors in the SRA, and the MCA energy, E_{MCA} , is determined by the force theorem,^{23–25} which is defined as the energy eigenvalue difference for the magnetization oriented along the in-plane [100] and the out-of-plane [001] directions. The use of 7056 special \mathbf{k} points in the two-dimensional Brillouin zone (BZ) was found to be sufficient to suppress numerical fluctuations in E_{MCA} .

As models of an ideal abrupt Fe/MgO interface, we consider two structures as shown in Fig. 1: (a) Fe/MgO(001) and (b) Au₃/Fe₃/MgO(001) structures. The first represents a surface Fe monolayer on an MgO(001) substrate and the latter, an Au-capped, three-atomic-layer Fe film on an MgO substrate where the surface magnetoelectric effect^{9,12} is eliminated by the nonmagnetic Au overlayer. The Fe atoms at the interface are on top of the O atoms, as found by first-principles calculations²⁶ and low-energy electron diffraction experiments.²⁷ In order to discuss the role of an interfacial

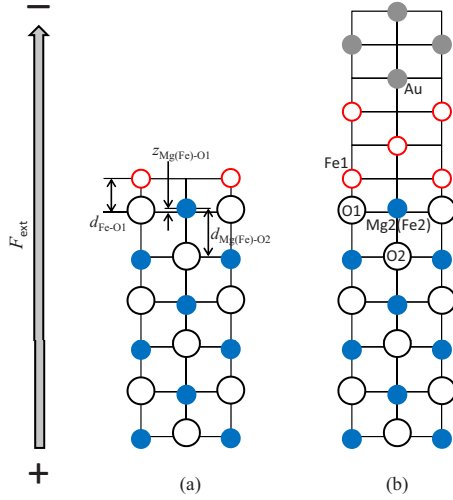


FIG. 1. (Color online) Models and notation for the atomic structures of an ideal Fe/MgO(001) interface: (a) Fe/MgO and (b) Au₃/Fe₃/MgO structures. The arrow at the left indicates the direction of the external electric field. An interfacial FeO layer between the Fe layer and the MgO substrate is modeled by replacing Mg atoms (Mg2) on the interface MgO layer by Fe atoms.

FeO_x layer between the Fe layer and the MgO substrate, we consider two additional structures, Fe/FeO_x/MgO and Au₃/Fe₃/FeO_x/MgO, where (for $x=1$) Mg atoms on the MgO interface layer (Mg2 atoms in Fig. 1) are replaced by Fe atoms. For each structure, the in-plane lattice constant is constrained to the calculated bulk MgO value. (The mismatch between MgO and Fe lattice constants is $\sim 4\%$.) The atomic z positions are fully optimized using the atomic-force FLAPW calculations,²⁸ including the contributions from the E field.

First, we present the atomic and the electronic structures of the Fe/MgO interfaces in zero field. Results for the interatomic distances between Fe1 and O1 atoms (cf. Fig. 1), $d_{\text{Fe-O1}}$, between Mg2 (Fe2) and O2 atoms, $d_{\text{Mg(Fe)-O2}}$, and the interlayer distance of Fe2 (Mg2) and O1 atoms, $z_{\text{Mg(Fe)-O1}}$, are summarized in Table I. For the ideal abrupt Fe/MgO interface of both Fe/MgO and Au₃/Fe₃/MgO structures, the structural parameters obtained are almost identical to each other with a small rumpling of the MgO layer (~ 0.1 Å of $z_{\text{Mg-O2}}$). However, as seen in Fe/FeO/MgO and Au₃/Fe₃/FeO/MgO structures, the existence of the interfacial FeO layer significantly decreases the interatomic distance $d_{\text{Fe-O1}}$ by 8%, indicating an enhancement of the hybridization between Fe1 and O1 atoms. Moreover, a large rumpling, i.e., a large outward displacement of the interfacial Fe2 atoms with respect to the O1 atoms (~ 0.3 Å of $z_{\text{Fe-O2}}$) is observed. Note that the calculated structural parameters qualitatively agree with those analyzed by surface x-ray diffraction.^{29,30}

Figure 2 shows the calculated density of states (DOS) in the MT spheres of the Fe1 atoms in zero field for Fe/MgO and Fe/FeO/MgO structures. For the Fe/MgO structure, the overall DOS is similar to that in a free-standing Fe monolayer:¹⁰ the DOS around E_F arises mainly from the minority-spin states while the majority-spin states are almost fully occupied and are located from -1 to -4 eV below E_F .

TABLE I. Calculated interatomic (interlayer) distances, d (z), in Å, between Fe and O atoms at the interfaces and MCA energy, E_{MCA} , in meV, in zero field.

	$d_{\text{Fe-O1}}$	$d_{\text{Mg(Fe)-O2}}$	$z_{\text{Mg(Fe)-O1}}$	E_{MCA}
Fe/MgO	2.09	2.16	0.08	1.28
Au ₃ /Fe ₃ /MgO	2.08	2.14	0.05	0.94
Fe/FeO/MgO	1.91	2.35	0.32	-0.18
Au ₃ /Fe ₃ /FeO/MgO	1.91	2.30	0.27	-0.56

The orbital-decomposed DOS indicates that the minority-spin $d_{xz,yz}$ ($m = \pm 1$) bands still cross E_F but the minority-spin d_{z^2} ($m=0$) bands are pushed up above E_F due to weak hybridization with the O1 p_z orbitals. For the Fe/FeO/MgO structure, however, the enhancement of the Fe-O hybridization due to the existence of the interfacial FeO layer pushes the $d_{xz,yz}$ bands to higher energy above E_F . For the Au-capped Fe systems, the trend in the electronic structure is the same, although the DOS (not shown in the figure) indicates that the bandwidth becomes wider due to the presence of the overlayer.

We now consider the MCA. Tables I and II give the calculated E_{MCA} values in zero field and ± 1 V/Å, respectively. In zero field, the E_{MCA} for the ideal abrupt interface of Fe/MgO and Au₃/Fe₃/MgO structures have very large positive values of 1.28 meV and 0.94 meV, respectively, indicating a strong out-of-plane MCA compared to that of the free-standing Fe monolayer.¹⁰ When an E field is introduced, the MCA is modified; for the Fe/MgO structure, a negative E field enhances the MCA by 0.15 meV while a positive one reduces it by 0.10 meV. However, for these fields, no magnetization switching from the out of plane to the in plane is realized. Even in the case of the Au₃/Fe₃/MgO structure, the modification of the MCA is very small, ~ 0.05 meV. Thus, E -field-driven MCA switching may be difficult to achieve for these systems.

In striking contrast, for Fe/FeO/MgO and Au₃/Fe₃/FeO/MgO structures, the E_{MCA} turn out to have negative values of -0.18 meV and -0.56 meV, respectively.

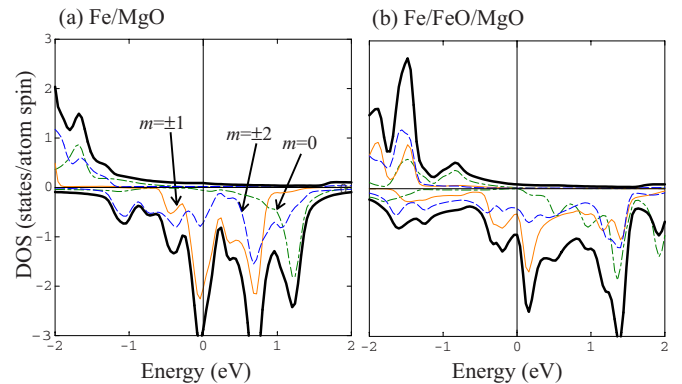


FIG. 2. (Color online) Zero-field DOS for Fe1 atoms (thick lines) for Fe/MgO and Fe/FeO/MgO structures along with the orbital-decomposed (thin lines) DOS. Dotted-dashed, solid, and dashed lines represent d_0 (d_{z^2}), $d_{\pm 1}$ ($d_{xz,yz}$), and $d_{\pm 2}$ ($d_{x^2-y^2,xy}$) orbitals, respectively.

TABLE II. Calculated interatomic (interlayer) distances, $d(z)$, between Fe and O atoms at the interfaces and MCA energy, E_{MCA} , in external electric fields of ± 1 V/Å. Notation is the same as in Table I.

	-1 V/Å				1 V/Å			
	$d_{\text{Fe-O1}}$	$d_{\text{Mg(Fe)-O2}}$	$z_{\text{Mg(Fe)-O1}}$	E_{MCA}	$d_{\text{Fe-O1}}$	$d_{\text{Mg(Fe)-O2}}$	$z_{\text{Mg(Fe)-O1}}$	E_{MCA}
Fe/MgO	2.07	2.12	0.03	1.43	2.10	2.17	0.10	1.18
Au ₃ /Fe ₃ /MgO	2.07	2.10	0.06	0.89	2.10	2.17	0.08	0.98
Fe/FeO/MgO	1.89	2.29	0.28	-0.07	1.93	2.43	0.36	-0.34
Au ₃ /Fe ₃ /FeO/MgO	1.90	2.25	0.23	-0.44	1.93	2.37	0.31	-0.80
Au ₃ /Fe ₃ /FeO _{0.5} /MgO	1.85	2.26	0.29	0.85	1.87	2.39	0.35	0.60

Thus, the presence of the interfacial FeO layer drastically changes the MCA. When an E field is introduced, a large MCA modification appears where a negative E field enhances the MCA by about 0.1 meV while a positive one reduces it by about 0.2 meV; this E field dependence is in agreement with experiments.^{15,16}

In order to understand the MCA, the minority-spin band structures and the MCA energy contributions, $E_{\text{MCA}}(\mathbf{k})$, in E fields of ± 1 V/Å along high-symmetry directions for Fe/MgO and Fe/FeO/MgO structures are shown in Fig. 3. For the Fe/MgO structure, the overall features of the d -band structure are not altered much compared to those of a free-standing Fe monolayer.¹⁰ However, since the d_z bands are pushed up above E_F [cf. Fig. 2(a)], the negative $E_{\text{MCA}}(\mathbf{k})$ around $\bar{\Gamma}$ (see Fig. 3 in Ref. 10) disappears, indicating that the out-of-plane MCA is enhanced compared to the free-standing Fe monolayer. Since there are no band intersections between d_{z^2} and $d_{xz,yz}$ bands at $\frac{1}{3}(\bar{\Gamma}-\bar{M})$ and $\frac{3}{5}(\bar{X}-\bar{\Gamma})$ around E_F , the MCA modification in these \mathbf{k} points is no longer excited when an E field is introduced. Thus, the modification of the MCA by an applied E field occurs only around \bar{M} as seen in Fig. 3(a).

Furthermore, for the Fe/FeO/MgO structure, the positive $E_{\text{MCA}}(\mathbf{k})$ around \bar{M} disappears since the $d_{xz,yz}$ bands shift to higher energy above E_F and do not cross E_F , as seen in Fig. 3(b). Thus, $E_{\text{MCA}}(\mathbf{k})$ turns out to be negative in most of the BZ except around $\bar{\Gamma}$, which arises from the SOC between occupied d_{xy} and unoccupied $d_{xz,yz}$ states. When an E field is introduced, $E_{\text{MCA}}(\mathbf{k})$ around $\bar{\Gamma}$ is found to be very sensitive to the atomic position of the interfacial Fe2 atoms. As shown in Table II, the Fe2 atoms move inward in a negative E field but outward in a positive one, while calculations with no atomic relaxation, i.e., fixing the structural parameters at the zero-field values, lead to a very small MCA modification (within 0.06 meV) for both Fe/FeO/MgO and Au₃/Fe₃/FeO/MgO structures, demonstrating the importance of the field-induced relaxations.

Based on these results, we conclude that at the ideal abrupt Fe/MgO interface the E -field-driven MCA switching from the out-of-plane MCA to the in-plane MCA does not occur, but rather the existence of an interfacial FeO layer between the metallic Fe layer and the MgO substrate plays a key role. For the Au-capped Fe systems, we estimate the dependence of E_{MCA} on the oxygen concentration in the interfacial FeO _{x} layer [cf. Fig. 4(a)], including additional calculations for Au₃/Fe₃/FeO_{0.5}/MgO where the $\sqrt{2} \times \sqrt{2}$ cell of Fig. 1(b) was employed. Results indicate that formation of the partial interfacial FeO layer enhances the MCA energy difference between positive and negative E fields compared to the ideal abrupt Fe/MgO interface and x in the range 50–100 % are promising candidate for E -field-driven MCA switching. The calculated structural parameters (given in Table II) are found to be roughly similar to those of Au₃/Fe₃/FeO/MgO, i.e., the Fe atoms in the interfacial FeO_{0.5} layer are displaced by the E field as well. Growth of such partial interfacial atomic structures might be possible by adjusting the oxygen atmosphere, as demonstrated in experiments^{29–31} and first-principles calculations.³²

E_{MCA} can also be modified by changing the number of valence electrons by, for example, doping with Co. The results for the Au-capped Fe systems within a rigid band model are shown in Fig. 4(b). For the interface with a FeO_{0.5} interfacial, the E_{MCA} in both positive and negative E fields decreases at approximately the same rate as the number of valence electrons increases. For approximately $\Delta N > 0.2$ electrons/Fe atom, switching should be feasible, consistent with recent experiments for the Au/FeCo/MgO.¹⁶ In contrast,

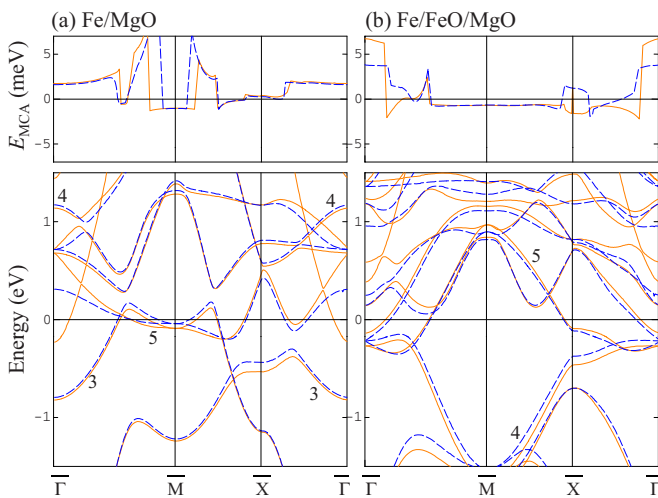


FIG. 3. (Color online) Calculated minority-spin band structures and MCA energy contribution, $E_{\text{MCA}}(\mathbf{k})$ along high-symmetry directions for (a) Fe/MgO and (b) Fe/FeO/MgO structures in external electric fields of -1 V/Å (dashed lines) and 1 V/Å (solid lines). Bands 3, 4, and 5 stand for $d_{x^2-y^2}$, d_{xy} , and $d_{xz,yz}$ states, respectively.

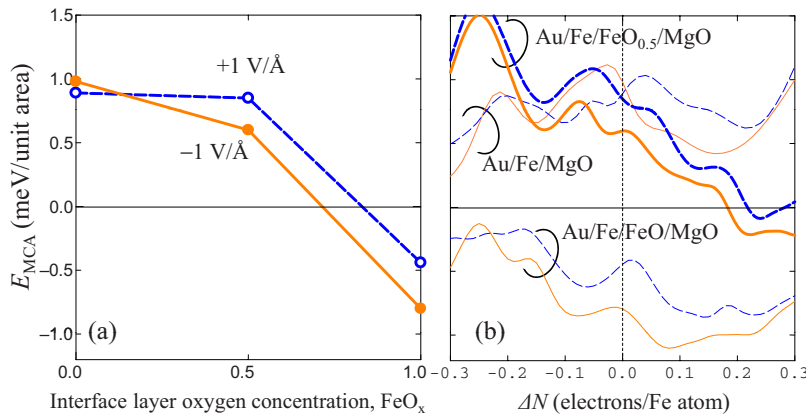


FIG. 4. (Color online) (a) Dependence of E_{MCA} on the oxygen concentration x in the interfacial FeO_x layer for the Au-capped Fe/MgO interfaces for external electric fields of 1 V/Å (open circles) and -1 V/Å (closed circles). (b) Calculated E_{MCA} as a function of the change in the number of valence electrons (ΔN) for the different systems. Dashed and solid lines represent results for an external electric field of 1 eV/Å and -1 eV/Å , respectively.

for both the ideal abrupt Fe/MgO interface and the interface with the perfect interfacial FeO layer, the E -field-driven MCA switching is unlikely, as shown in Fig. 4(b).

We thank R. Shimabukuro for fruitful discussions. Work at Mie University was supported by a Grant-in-Aid for Scientific Research (Grant No. 20540334) from the Japan Soci-

ety for the Promotion of Science and for computations partially performed at ISSP, University of Tokyo. Work at Northwestern University (Grant No. DE-FG02-88ER45372) and the University of Wisconsin–Milwaukee (Grant No. DE-FG02-06ER46328) was supported by the U.S. Department of Energy.

*kohji@phen.mie-u.ac.jp

- ¹M. Fiebig, *J. Phys. D* **38**, R123 (2005), and references therein.
- ²W. Eerenstein, W. Mathur, and J. F. Scott, *Nature (London)* **442**, 759 (2006), and references therein.
- ³R. Ramesh and N. A. Spaldin, *Nature Mater.* **6**, 21 (2007), and references therein.
- ⁴Y. Tokura, *J. Magn. Magn. Mater.* **310**, 1145 (2007), and references therein.
- ⁵H. Ohno, D. Chiba, F. Matsukura, T. Omiya, E. Abe, T. Dietl, Y. Ohno, and K. Ohtanis, *Nature (London)* **408**, 944 (2000).
- ⁶D. Chiba, M. Yamanouchi, F. Matsukura, and H. Ohno, *Science* **301**, 943 (2003).
- ⁷D. Chiba, M. Sawicki, Y. Nishitani, Y. Nakatani, F. Matsukura, and H. Ohno, *Nature (London)* **455**, 515 (2008).
- ⁸M. Weisheit, S. Fähler, A. Marty, Y. Souche, C. Poinshignon, and D. Givord, *Science* **315**, 349 (2007).
- ⁹C.-G. Duan, J. P. Velev, R. F. Sabirianov, Z. Zhu, J. Chu, S. S. Jaswal, and E. Y. Tsymlal, *Phys. Rev. Lett.* **101**, 137201 (2008).
- ¹⁰K. Nakamura, R. Shimabukuro, Y. Fujiwara, T. Akiyama, T. Ito, and A. J. Freeman, *Phys. Rev. Lett.* **102**, 187201 (2009).
- ¹¹M. Tsujikawa and T. Oda, *Phys. Rev. Lett.* **102**, 247203 (2009).
- ¹²K. Nakamura, R. Shimabukuro, T. Akiyama, T. Ito, and A. J. Freeman, *Phys. Rev. B* **80**, 172402 (2009).
- ¹³J. S. Moodera and G. Mathon, *J. Magn. Magn. Mater.* **200**, 248 (1999), and references therein.
- ¹⁴W. H. Butler, X.-G. Zhang, T. C. Schulthess, and J. M. MacLaren, *Phys. Rev. B* **63**, 054416 (2001).
- ¹⁵T. Maruyama, K. Ohta, T. Nozaki, T. Shinjo, M. Shiraishi, S. Mizukami, Y. Ando, and Y. Suzuki, *Nat. Nanotechnol.* **4**, 158 (2009).
- ¹⁶Y. Shiota, T. Maruyama, T. Nozaki, T. Shinjo, M. Shiraishi, and

Y. Suzuki, *Appl. Phys. Express* **2**, 063001 (2009).

- ¹⁷E. Wimmer, H. Krakauer, M. Weinert, and A. J. Freeman, *Phys. Rev. B* **24**, 864 (1981).
- ¹⁸M. Weinert, E. Wimmer, and A. J. Freeman, *Phys. Rev. B* **26**, 4571 (1982).
- ¹⁹M. Weinert, G. Schneider, R. Podloucky, and J. Redinger, *J. Phys.: Condens. Matter* **21**, 084201 (2009).
- ²⁰U. von Barth and L. Hedin, *J. Phys. C* **5**, 1629 (1972).
- ²¹R. Wu and A. J. Freeman, *J. Magn. Magn. Mater.* **200**, 498 (1999).
- ²²C. Li, A. J. Freeman, H. J. F. Jansen, and C. L. Fu, *Phys. Rev. B* **42**, 5433 (1990).
- ²³M. Weinert, R. E. Watson, and J. W. Davenport, *Phys. Rev. B* **32**, 2115 (1985).
- ²⁴G. H. O. Daalderop, P. J. Kelly, and M. F. H. Schuurmans, *Phys. Rev. B* **41**, 11919 (1990).
- ²⁵X. D. Wang, D. S. Wang, R. Q. Wu, and A. J. Freeman, *J. Magn. Magn. Mater.* **159**, 337 (1996).
- ²⁶C. Li and A. J. Freeman, *Phys. Rev. B* **43**, 780 (1991).
- ²⁷T. Urano and T. Kanaji, *J. Phys. Soc. Jpn.* **57**, 3403 (1988).
- ²⁸R. Yu, D. Singh, and H. Krakauer, *Phys. Rev. B* **43**, 6411 (1991).
- ²⁹H. L. Meyerheim, R. Popescu, N. Jedrecy, M. Vedpathak, M. Sauvage-Simkin, R. Pinchaux, B. Heinrich, and J. Kirschner, *Phys. Rev. B* **65**, 144433 (2002).
- ³⁰C. Tusche, H. L. Meyerheim, N. Jedrecy, G. Renaud, and J. Kirschner, *Phys. Rev. B* **74**, 195422 (2006).
- ³¹H. L. Meyerheim, R. Popescu, J. Kirschner, N. Jedrecy, M. Sauvage-Simkin, B. Heinrich, and R. Pinchaux, *Phys. Rev. Lett.* **87**, 076102 (2001).
- ³²B. D. Yu and J.-S. Kim, *Phys. Rev. B* **73**, 125408 (2006).